Stick-Slip Motion Control for an Orthogonal-Type Robot

F. Nagata, T. Mizobuchi, S. Tani
Tokyo University of Science, Yamaguchi
Sanyo-Onoda, Japan

T. Hase, Z. Haga
R&D Center, Meiho Co. Ltd.
Nogata, Japan

K. Watanabe
Okayama University
Okayama, Japan

Maki K. Habib
American University in Cairo
Cairo, Egypt

Abstract

In this paper, a new desktop orthogonal-type robot, which has abilities of compliant motion and stick-slip motion, is presented for lapping small metallic molds with curved surface. The robot consists of three single-axis devices with a high position resolution of 1 μm. A thin wood stick tool is attached to the tip of the z-axis. The tool tip has a small ball-end shape. In order to improve the lapping performance, a small stick-slip motion control is considered in the control system. The small stick-slip motion is orthogonally generated to the direction of the tool's moving direction. The effectiveness of the stick-slip motion control is examined through an actual lapping test of an LED lens mold with a diameter of 4 mm.

1 Introduction

In manufacturing process of small lens molds such as an LED lens and pickup lens, 3D CAD/CAM systems and NC machining centers are used generally, and these advanced systems have rationalized the design and manufacturing process. However, the finishing process called the lapping after machining process has been hardly automated yet, because an LED lens mold has plural small concave areas to be finished. That means the target mold is not axis-symmetric. Almost conventional effective polishing systems can deal with axis-symmetric workpieces but cannot be applied to such an LED lens mold. In other words, no effective finishing systems have been successfully developed for axis-asymmetric LED lens molds. For example, Tsai et al. developed a mold polishing robot [1] and its path planning technique [2], however, the applicability to small axis-asymmetric LED lens molds was not described. Also, we could not find out other previous literature concerning the finishing of axis-asymmetric LED lens molds. Actually, axis-asymmetric LED lens molds are manually finished by skilled workers in almost all cases.

In this paper, a new desktop orthogonal-type robot, which has abilities of compliant motion and stick-slip motion, is first presented for lapping small metallic molds with curved surface. The robot consists of three single-axis devices with a high position resolution of 1 μm. A thin wood stick tool is attached to the tip

of the z-axis. The tool tip has a small ball-end shape. The control system is composed of a force feedback loop, position feedback loop and position feedforward loop. The force feedback loop controls the polishing force consisting of tool contact force and kinetic friction forces. The position feedback loop controls the position in pick feed direction, e.g., z-direction. The position feedforward loop leads the tool tip along a desired trajectory called cutter location data (CL data). The CL data are generated from the main-processor of a CAM system. The proposed robot has realized a compliant motion required for the surface following control along a spiral path.

In order to improve the finishing performance, a small stick-slip motion control strategy is further added to the control system. The small stick-slip motion is orthogonally generated to the direction of the tool's moving direction. Generally, the stick-slip motion is an undesirable phenomenon and should be eliminated in precision machineries [3, 4]. However, the proposed robot employs a small stick-slip motion to improve the lapping quality. The effectiveness of the robot with the ability of stick-slip motion is examined through an actual lapping test of an LED lens mold with a diameter of 4 mm. It is expected due to the abilities of compliant motion and stick-slip motion that the undesirable small cusps can be uniformly removed and the robot has an effectiveness to achieve a higher quality surface like a mirror finishing.

2 Desktop Orthogonal-Type Robot

Figure 1 shows the developed desktop orthogonal-type robot consisting of three single-axis devices with position resolution of 1 μm. The size is 850 $\times$ 645 $\times$ 700 mm. The single-axis device is a position control robot ISPA with high-precision resolution provided by IAI Corp., which is composed of a base, linear guide, ball-screw, AC servo motor. The effective strokes in x-, y- and z-directions are 400, 300 and 100 mm, respectively. The tool axis is designed to be parallel to z-axis of the robot. A wood stick tool is fixed to the tip through a 3-DOF compact force sensor. To regulate the rotation, a servo spindle is located parallel to the tool axis. The position resolution and force resolu-
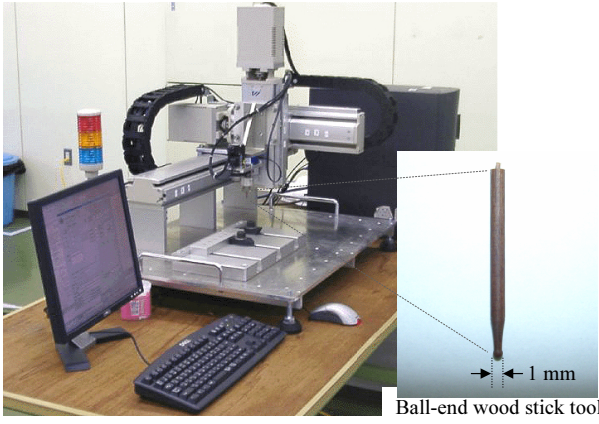
Figure 1: Proposed desktop orthogonal-type robot with compliance control capability.
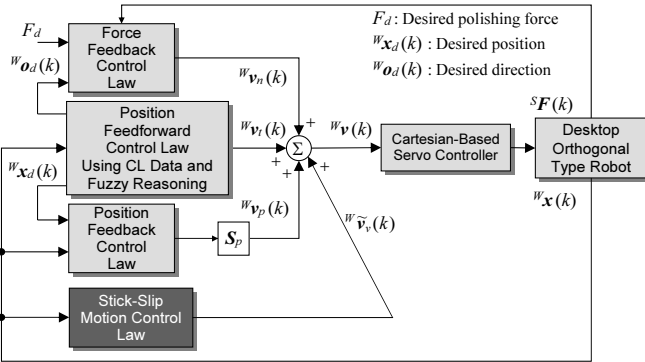
Figure 2: Position/force controller with stick-slip motion control method.

tion, and effective stiffness at the tool tip were examined through a simple contact experiment, so that the force resolution of 0.178 N was obtained due to the position resolution of 1 μm. Therefore, the effective stiffness can be estimated about 178 N/mm.

3 Basic Position/Force Control

The basic lapping strategy is conducted along a continuous spiral path while performing a stable polishing force [5]. In this section, the control system is briefly explained. The tool tip is controlled by the translational velocity $^W\boldsymbol{v}(k) = [^Wv_x(k)\ ^Wv_y(k)\ ^Wv_z(k)]^T$ given by

$$^W\boldsymbol{v}(k) = {}^W\boldsymbol{v}_t(k) + {}^W\boldsymbol{v}_n(k) + {}^W\boldsymbol{v}_p(k) \tag{1}$$

where k denotes the discrete time; superscript ^{W} denotes the work coordinate system. Note that the control system easily realized 1 msec sampling time by using the Windows multimedia timer. It is assumed that the polishing force is the resultant force of the contact force and kinetic friction forces, and is obtained as the resultant force of x-, y- and z-directional force sensor measurements. Figure 2 shows the proposed position/force controller with the stick-slip motion control. First of all, $^W\boldsymbol{v}_t(k)$ is the manipulated variable generated from the feedforward control law based on cutter location data called the CL data. $^W\boldsymbol{v}_t(k)$ is the tangential velocity and written by
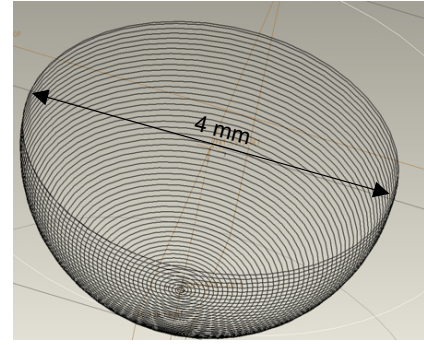
Figure 3: Spiral path generated by using the main-processor of the CAM, which is used for the desired trajectory of the wood stick tool.

$$^W\boldsymbol{v}_t(k) = v_{tangent}(k)\frac{^W\boldsymbol{t}(k)}{\|^W\boldsymbol{t}(k)\|} \tag{2}$$

where $v_{tangent}(k)$ is a velocity scalar. $^W\boldsymbol{t}(k)$ is the tangential vector calculated by the CL data. Also, $^W\boldsymbol{v}_n(k)$ is the manipulated variable generated from the force feedback control law. $^W\boldsymbol{v}_n(k)$ is the normal velocity and written by

$$^W\boldsymbol{v}_n(k) = v_{normal}(k)^W\boldsymbol{o}_d(k) \tag{3}$$

where $^W\boldsymbol{o}_d(k)$ is the normalized normal direction vector calculated by using the CL data. The scalar $v_{normal}(k)$ representing the normal velocity is the output of the impedance model following force control law [5] given by

$$v_{normal}(k) = v_{normal}(k-1)e^{-\frac{B_d}{M_d}\Delta t}$$
$$+ \left(e^{-\frac{B_d}{M_d}\Delta t} - 1\right)\frac{K_f}{B_d}E_f(k) \tag{4}$$

where K_f is the force feedback gain, and impedance parameters M_d and B_d are the desired mass and damping coefficients, respectively. Δt is the sampling time. Also, $E_f(k)$ is the error between the desired polishing force F_d and norm of force $^S\boldsymbol{F}(k) \in \Re^3$ measured by the force sensor, which is written by

$$E_f(k) = F_d - \|^S\boldsymbol{F}(k)\| \tag{5}$$

where superscript ^{S} represents the sensor coordinate system. Further, $^W\boldsymbol{v}_p(k)$ is the manipulated variable yielded by a position feedback control law given by

$$^W\boldsymbol{v}_p(k) = \boldsymbol{S}_p\Big\{\boldsymbol{K}_p\boldsymbol{E}_p(k) + \boldsymbol{K}_i\sum_{n=1}^{k}\boldsymbol{E}_p(n)\Big\} \tag{6}$$

where the switch matrix $\boldsymbol{S}_p = \mathrm{diag}(S_x, S_y, S_z)$ makes the weak coupling control to the force control active or inactive in each direction; $\boldsymbol{E}_p(k) = {}^W\boldsymbol{x}_d(k) - {}^W\boldsymbol{x}(k)$ is the position error. The desired position $^W\boldsymbol{x}_d(k)$ is calculated by using CL data. $\boldsymbol{K}_p = \mathrm{diag}(K_{px}, K_{py}, K_{pz})$ and $\boldsymbol{K}_i = \mathrm{diag}(K_{ix}, K_{iy}, K_{iz})$ are proportional and integral gains for position feedback control. Due to the weak coupling control, it is simultaneously realized that stable polishing force control and profiling control along a spiral path.

Next, the proposed system is applied to the finishing of an LED lens mold. Figure 3 shows the spiral
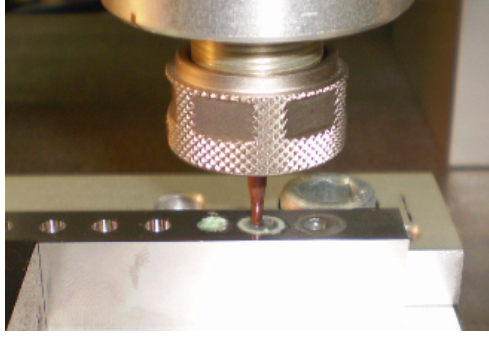
Figure 4: Lapping scene by using the proposed robot, in which a special oil including diamond lapping paste is poured.

Before lapping   After lapping
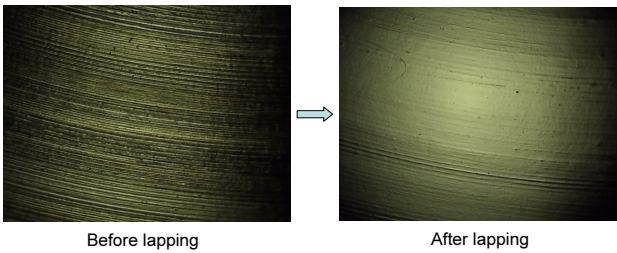
Figure 5: Finished surface before and after the lapping process.

path generated from the main-processor of the CAM, which is used in the lapping experiment. The spiral path has position and orientation components. Figure 4 shows the lapping scene of the LED lens mold, where a special oil including the diamond lapping paste is poured. In this case, a small ball-end tool lathed from a wood stick is used, whose tip diameter is 1 mm. Figure 5 shows large scale photos of the surfaces before and after the lapping process. It is observed that the undesirable cusps still remain on the surface of concaved area.

4   Stick-Slip Motion Control

In this section, the effectiveness of the tool's stick-slip motion is evaluated to improve the surface quality. Generally, the stick-slip motion is an undesirable phenomenon and should be eliminated in various precise machine tools. However, the proposed orthogonal-type robot employs a small stick-slip motion not only to improve the finishing quality but also to skillfully emphasize the polishing energy. Figure 6 shows a simple image of the stick-slip motion seen like small vibrations. The stick-slip motion is given along curved surface and also to orthogonal directions of tool's profiling velocity $^{W}\boldsymbol{v}_t(k)$. Here, how to generate small stick-slip motion vectors is explained in detail by using Fig. 7. In Fig. 7, point O is the origin in work coordinate system, where the tool tip initially contacts the workpiece. Point P is the current contact point. $^{W}\boldsymbol{x}(k)$ is the position vector given by $^{W}\boldsymbol{x}(k) = [^{W}x(k) \ ^{W}y(k) \ ^{W}z(k)]^T$ viewed from O; $^{W}\boldsymbol{o}_d$ is the normalized normal vector at the
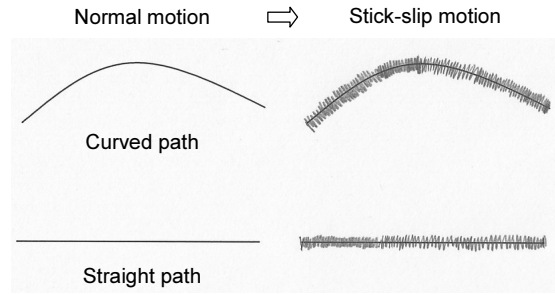
Figure 6: Image of the small stick-slip motion.
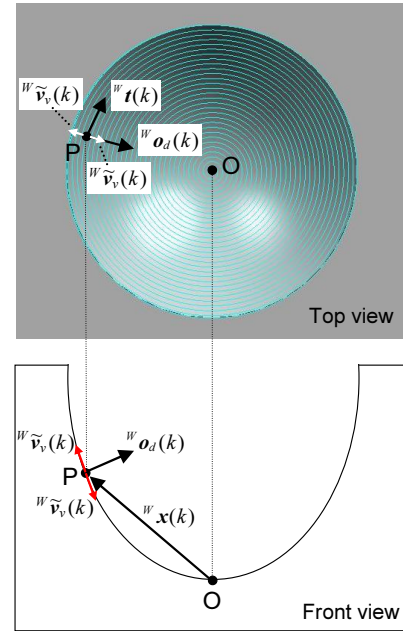
Figure 7: Calculation of stick-slip motion vector

point P given by $^{W}\boldsymbol{o}_d = [^{W}o_{dx}(k) \ ^{W}o_{dy}(k) \ ^{W}o_{dz}(k)]$; $^{W}\boldsymbol{t}(k) = [^{W}t_x(k) \ ^{W}t_y(k) \ ^{W}t_z(k)]^T$ is the tangential vector at the point P. Here, it is assumed that $^{W}\boldsymbol{v}_v(k) = [^{W}v_{vx}(k) \ ^{W}v_{vy}(k) \ ^{W}v_{vz}(k)]^T$ is a small stick-slip vector to be calculated.

In this example, the tool approaches to the workpiece with a low speed and follow the spiral path after contacting the point O. Because $^{W}\boldsymbol{v}_v(k)$ is perpendicular to $^{W}\boldsymbol{o}_d(k)$, the following relation is obtained.

$$^{W}v_{vx}(k) \ ^{W}o_{dx}(k) + ^{W}v_{vy}(k) \ ^{W}o_{dy}(k)$$
$$+^{W}v_{vz}(k) \ ^{W}o_{dz}(k) = 0 \qquad (7)$$

Also, $^{W}\boldsymbol{v}_v(k)$ and $^{W}\boldsymbol{t}(k)$ are orthogonal each other, so that

$$^{W}v_{vx}(k) \ ^{W}t_x(k) + ^{W}v_{vy}(k) \ ^{W}t_y(k)$$
$$+^{W}v_{vz}(k) \ ^{W}t_z(k) = 0 \qquad (8)$$

Further, $^{W}\boldsymbol{v}_v(k)$ is located in a plane which includes both $^{W}\boldsymbol{o}_d(k)$ and $^{W}\boldsymbol{x}(k)$, so that the components of $^{W}\boldsymbol{v}_v(k)$ are represented by

$$^{W}v_{vx}(k) = i \ ^{W}o_{dx}(k) + j \ ^{W}x(k) \qquad (9)$$

$$^{W}v_{vy}(k) = i \,^{W}o_{dy}(k) + j \,^{W}y(k) \qquad (10)$$

$$^{W}v_{vz}(k) = i \,^{W}o_{dz}(k) + j \,^{W}z(k) \qquad (11)$$

where i and j are real numbers. By solving the Eqs. (7), (8), (9), (10) and (11), $^{W}v_{vx}(k)$, $^{W}v_{vy}(k)$ and $^{W}v_{vz}(k)$ can be obtained. Here, however, a simpler calculation is considered. First of all, substituting Eqs. (9), (10) and (11) into Eq. (7) and considering $\|^{W}\boldsymbol{o}_d(k)\|=1$ lead to

$$i = -j\{^{W}o_{dx}(k) \,^{W}x(k) + ^{W}o_{dy}(k) \,^{W}y(k) \\ + ^{W}o_{dz}(k) \,^{W}z(k)\} \qquad (12)$$

Accordingly, by giving Eq. (12) into Eqs. (9), (10) and (11), the following equations are obtained.

$$^{W}v_{vx}(k) = j\{^{W}x(k) - (^{W}o_{dx}(k) \,^{W}x(k) \\ + ^{W}o_{dy}(k) \,^{W}y(k) + ^{W}o_{dz}(k) \,^{W}z(k)) \,^{W}o_{dx}(k)\} \quad (13)$$

$$^{W}v_{vy}(k) = j\{^{W}y(k) - (^{W}o_{dx}(k) \,^{W}x(k) \\ + ^{W}o_{dy}(k) \,^{W}y(k) + ^{W}o_{dz}(k) \,^{W}z(k)) \,^{W}o_{dy}(k)\} \quad (14)$$

$$^{W}v_{vz}(k) = j\{^{W}z(k) - (^{W}o_{dx}(k) \,^{W}x(k) \\ + ^{W}o_{dy}(k) \,^{W}y(k) + ^{W}o_{dz}(k) \,^{W}z(k)) \,^{W}o_{dz}(k)\} \quad (15)$$

Because both $^{W}\boldsymbol{o}_d(k)$ and $^{W}\boldsymbol{x}(k)$ are known, $^{W}\boldsymbol{v}_v(k)$ can be normalized as $\boldsymbol{v}_v(k)/\|\boldsymbol{v}_v(k)\|$. Further, by using a scalar K_v and a sign $\text{SIGN}(k)$, the stick-slip motion vector is finally obtained as

$$^{W}\tilde{\boldsymbol{v}}_v(k) = \text{SIGN}(k) \, K_v \, \frac{\boldsymbol{v}_v(k)}{\|\boldsymbol{v}_v(k)\|} \qquad (16)$$

where $\text{SIGN}(k)$ is given by

$$\text{SIGN}(k) = \begin{cases} 1 & \text{if } k = \text{odd number} \\ -1 & \text{otherwise} \end{cases} \qquad (17)$$

$^{W}\tilde{\boldsymbol{v}}_v(k)$ is a velocity vector to yield another polishing energy, and which is given to the tool alternatively changing the direction every sampling period. The stick-slip motion control is simply added as shown in Fig. 2. As can be seen from Eqs. (2) and (3), the directions of $^{W}\boldsymbol{v}_t(k)$ and $^{W}\boldsymbol{v}_n(k)$ are the same ones of $^{W}\boldsymbol{t}(k)$ and $^{W}\boldsymbol{o}_d(k)$, respectively. Also, $^{W}\boldsymbol{v}_p(k)$ is generated in the direction of z-axis called the spiral direction.

Next, the effectiveness of the stick-slip motion control is examined through a same lapping experiment conducted in the previous section. Figure 8 shows the large scale photo of the LED lens mold after the lapping process by using the proposed stick-slip motion control. It is observed that the undesirable remained cusps can be removed uniformly. It has been confirmed from the result that the proposed finishing strategy by using the stick-slip motion control has a significant effectiveness to achieve a higher quality surface.

5 Conclusions

The final goal of this study is the development of a novel orthogonal-type robot with compliance controllability that can be applied to from the cusp mark removing process to the finishing process for mirror-like

Without Stick-slip motion   With Stick-slip motion
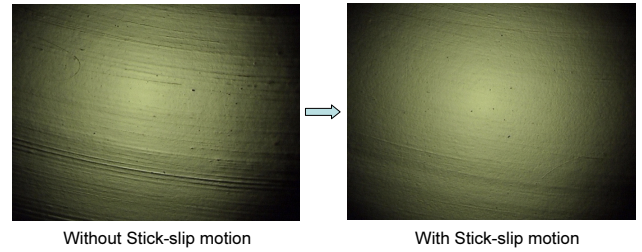
Figure 8: Large scale photos without and with by using the proposed stick-slip motion.

surface of LED lens molds. In this paper, a desktop orthogonal-type robot was first designed by combining three single-axis devices. The position resolution and force resolution, and effective stiffness are 1 μm, 0.178 N and 178 N/mm, respectively. Next, a basic position/force controller with compliance controllability was proposed for the lapping task of LED lens molds, in which position control, force control or their weak coupling control can be selected independently. Further, a stick-slip motion control for a wood stick tool was developed to finely improve the finishing quality. The proposed desktop orthogonal-type robot using the stick-slip motion control was applied to a lapping experiment of an LED lens mold, so that the high performance and promise were successfully confirmed. In future work, we plan to consider other potential applications using the robot.

References

[1] M. J. Tsai, J. L. Chang and J. F. Haung, "Development of an Automatic Mold Polishing System," *Procs. of 2003 IEEE Int. Conf.on Robotics & Automation*, pp. 3517–3522, Taipei, Taiwan, 2003.

[2] M. J. Tsai, J. J. Fang and J. L. Chang, "Robotic Path Planning for an Automatic Mold Polishing System, *International Journal of Robotics and Automation*, vol. 19, no. 2, pp. 81–89, 2004.

[3] O. Bilkay and O. Anlagan, "Computer Simulation of Stick-Slip Motion in Machine Tool Slideways," *Tribology International*, vol. 37, no. 4, pp. 347–351, 2004.

[4] X. Mei, M. Tsutsumi, T. Tao and N. Sun, "Study on the Compensation of Error by Stick-Slip for High-Precision Table," *International Journal of Machine tools & Manufacture*, vol. 44, no. 5, pp. 503–510, 2004.

[5] F. Nagata, T. Hase, Z. Haga, M. Omoto and K. Watanabe, "CAD/CAM-Based Position/Force Controller for a Mold Polishing Robot," *Mechatronics*, vol. 17, no. 4–5, pp. 207–216, 2007.